Supplementary Information

Enhancement of interlayer exchange coupling via intercalation in 2D magnetic bilayers: Towards high Curie temperature

Suman Mishra,[a] In Kee Park,[b] Saqib Javaid,[b,c] Seung Hwan Shin,[d,*] Geunsik Lee[a,b,*]

[a]*Department of Physics, Ulsan National Institute of Science and Technology, Ulsan 44919, Republic of Korea*

[b]*Department of Chemistry, Ulsan National Institute of Science and Technology, Ulsan 44919, Republic of Korea*

[c]*MMSG, Theoretical Physics Division, PINSTECH, P.O. Nilore, Islamabad, Pakistan*

[d]*Department of Accelerator Science, Korea University, Sejong 30019, Republic of Korea*

Correspondence and requests for materials should be addressed to S.H.S. (email: tlssh@korea.ac.kr) and G.L. (email: gslee@unist.ac.kr).

This supplementary information includes:

Note1

Figures: S1-S11

Tables: S1-S7

Note1. Thermal and dynamical stability of Ni@bi-CrI_3 and Cr@bi-NiI_2

Figure S5(a) presents variation of MD potential energy as a function of time step for Ni@bi-CrI_3. As evident, after equilibration, the potential energy oscillates around mean value, and no significant drop is observed for the whole length of the simulations (10 ps). This underscores the thermal stability of Ni@bi-CrI_3. Similarly, the phonon dispersion spectra as retrieved from QMD simulations confirm the absence of any imaginary frequencies. Therefore, we conclude that Ni@bi-CrI_3 is a stable structure. Similar results are also found for Cr@bi-NiI_2 as shown in figure S5(b), except for some small negative frequencies around Γ-point. However, such small negative frequencies around Γ-point can be found in the case of 2D materials [3] as consequence of numerical issues [4] rather than actual dynamical instability. We note further that the phonon spectra have been retrieved from MD trajectory at T= 300 K, to model realistic experimental conditions by employing TDEP code. However, acoustic sum rules are currently not implemented in TDEP, which may also lead to unphysical negative frequencies at Γ-point. Overall, these findings clearly show that both Ni@bi-CrI_3 and Cr@bi-NiI_2 satisfy the key stability criteria for 2D materials.

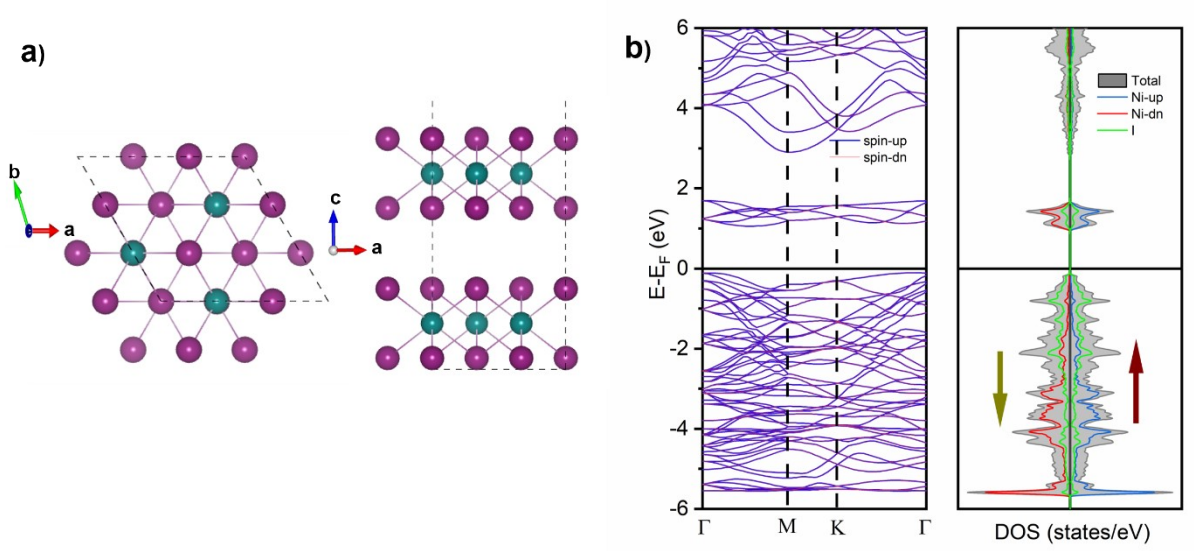

Figure S1. Optimized crystal structure and electronic properties of √3×√3 bi-NiI_2. (a) Top view and side view in left and right panels. **(b)** Represents band structure and DOS.

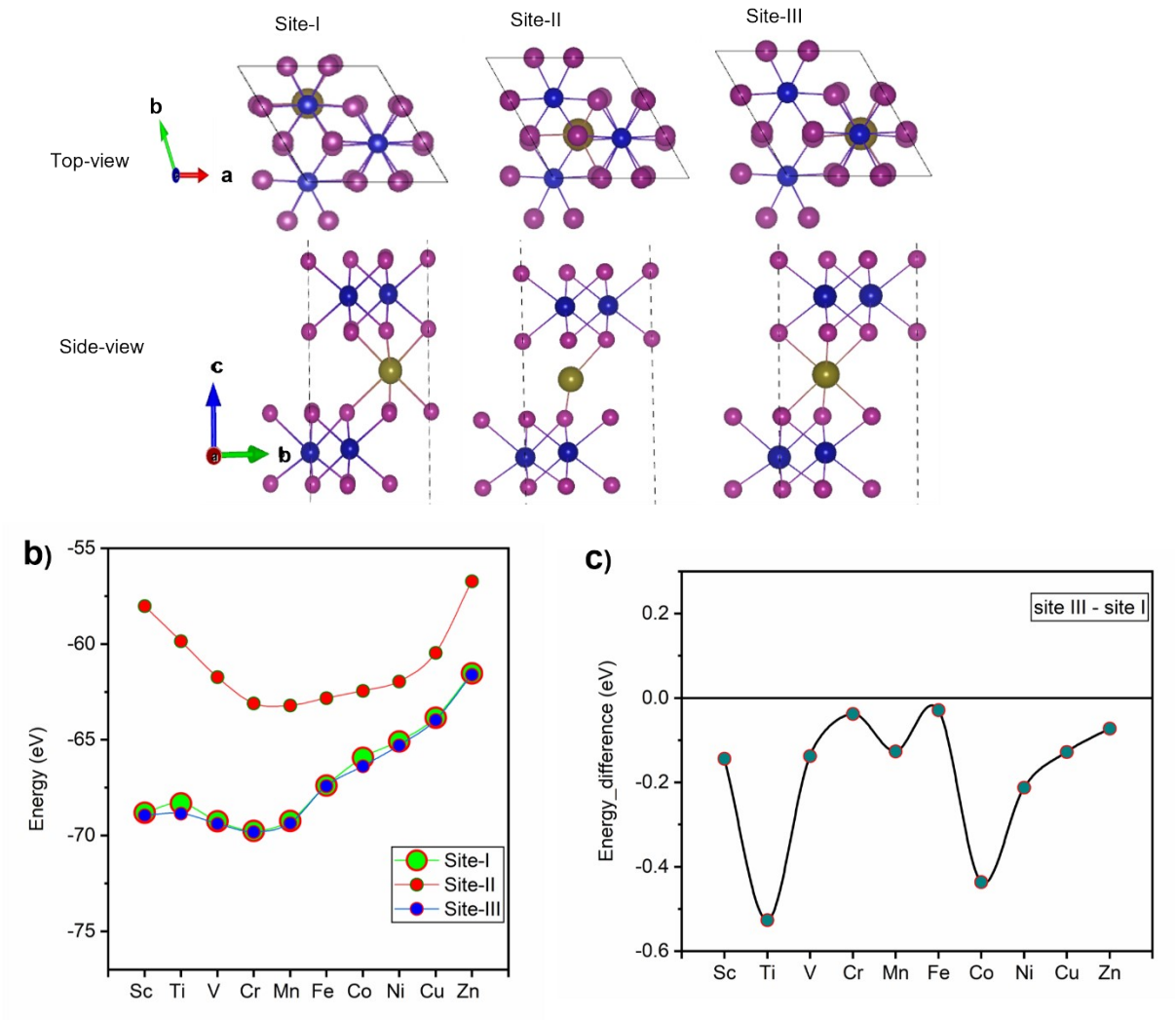

Figure S2. Sites used for TM intercalation and their energies in TM@bi-CrI_3. **(a)** Three different sites, I (TM is at the top position of Cr atom of one layer and hollow position of the other layer), II (In between Iodine atoms of both layers) and III (in between Cr atoms of both layers) have been used to check most stable site for intercalation, upper panel is top view and lower panel is the side view of TM@bi-CrI_3 for different sites. **(b)** Shows the total energies of different sites. Site II is energetically most unstable one. However, sites I and III have comparable energies. **(c)** Energy difference between site I and III. Shows that site III is energetically more favourable than both site I and site II.

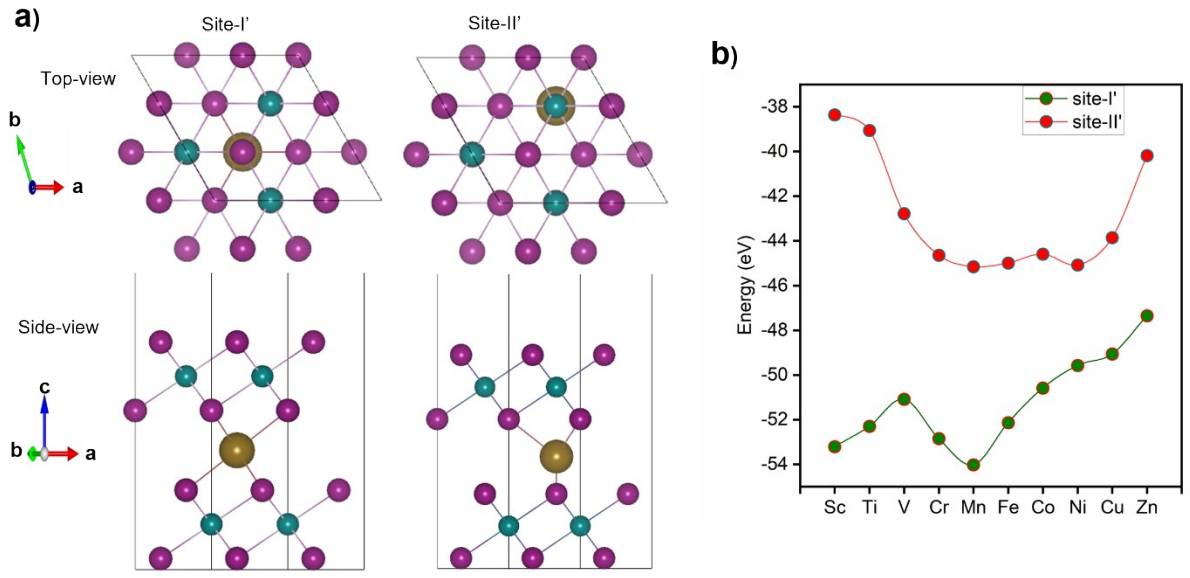

Figure S3. Sites used for TM intercalation and their energies in √3×√3 bi-NiI_2. (a) Two different sites I' (In between Iodine atoms of two layers) and II' (between Iodine and Ni atoms of two layers) have been used to check most stable site for intercalation, upper panel is top view and lower panel is the side view. **(b)** Shows the total energies of different sites. Site I' is energetically more stable than site II'.

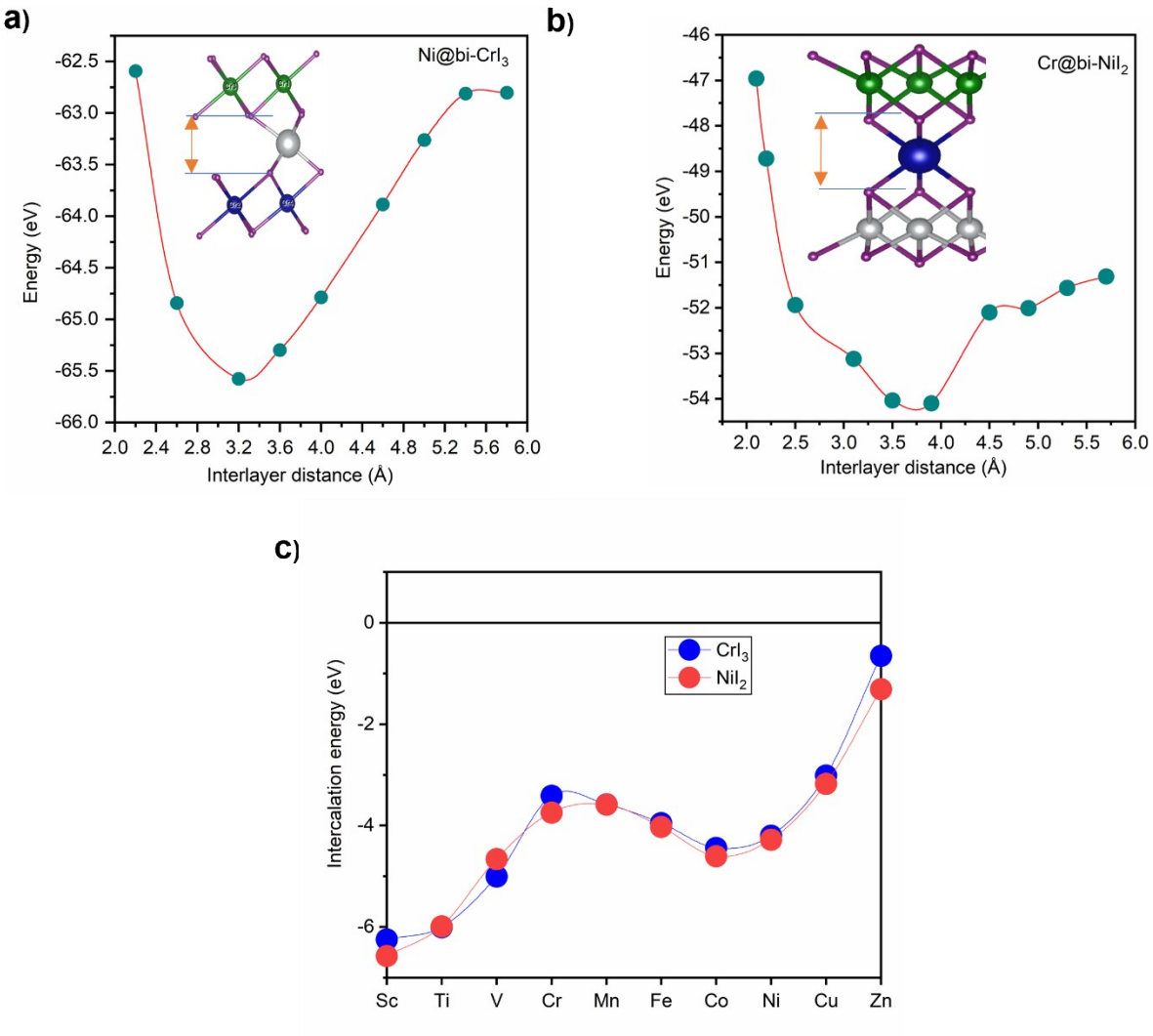

Figure S4. Interlayer energy. Total energies versus interlayer distance denoted by the arrow in the inset for **(a)** Ni@bi-CrI_3, **(b)** $\sqrt{3}\times\sqrt{3}$ Cr@bi-NiI_2. **(c)** Intercalation energy according to $E_{int} = E_{TM@BL} - E_{BL} - E_{TMA}$, where E_{TMA} is the energy of an isolated TM atom, showing that all TM intercalations are energetically favourable against agglomeration.

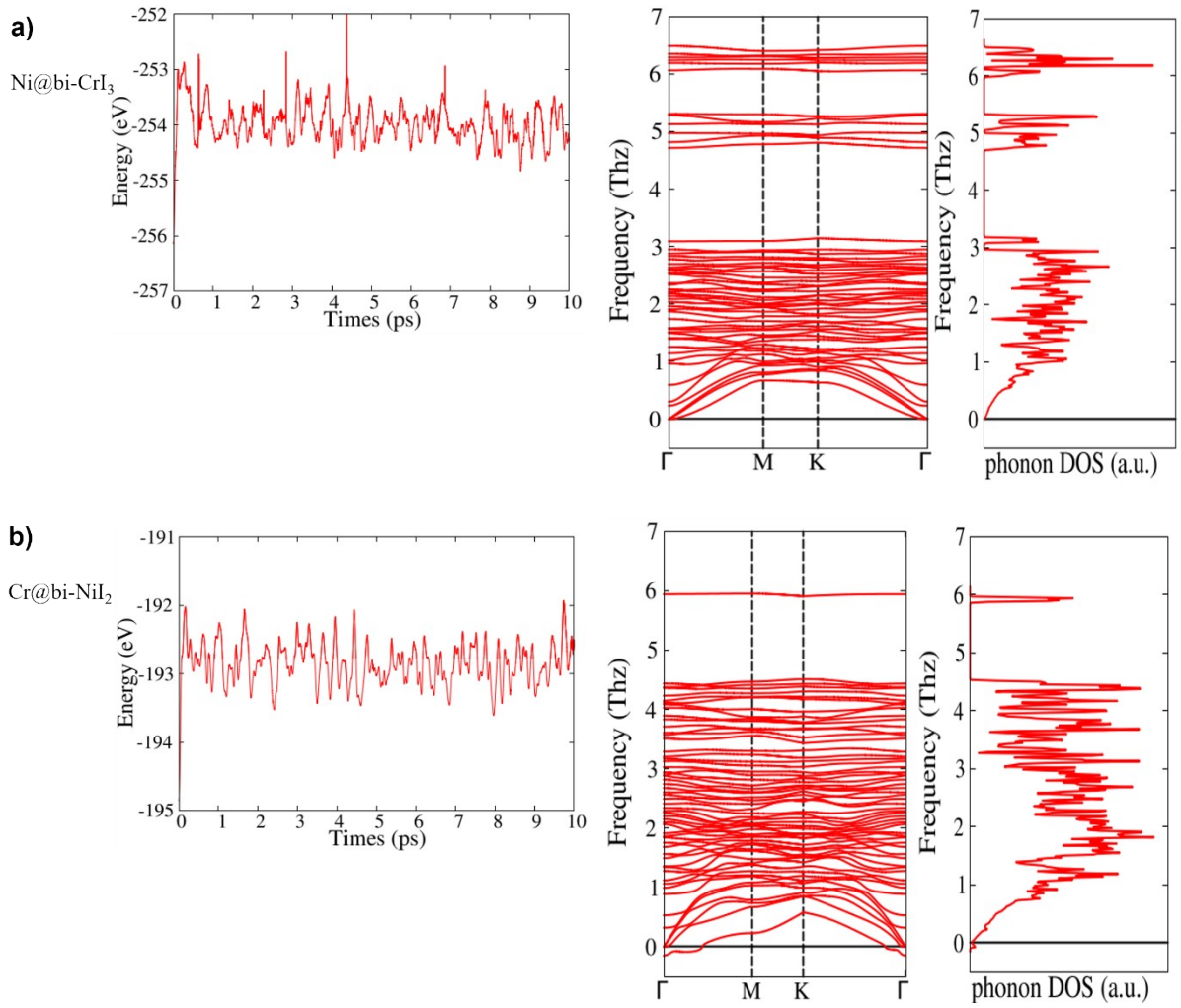

Figure S5. MD simulation and phonon data (a) Ni@bi-CrI_3**. (b)** Cr@bi-NiI_2**.**

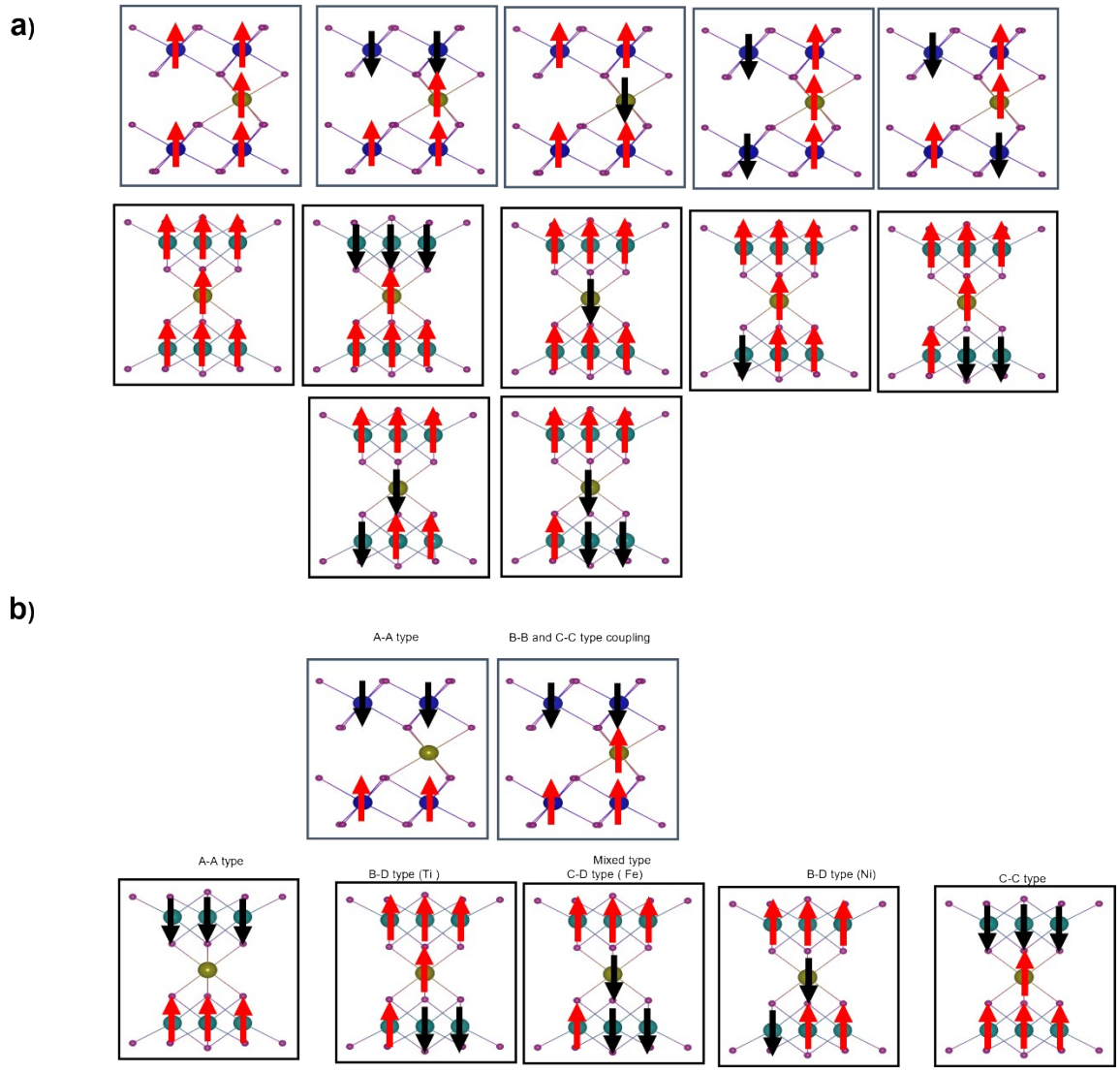

Figure S6. Magnetic configurations (a) Various magnetic configurations of TM@bi-CrI_3 that has been used to check most stable magnetic ground state, upper panel and TM@bi-NiI_2 two lower panels. **(b)** AFM states for different type of coupling in TM@bi-CrI_3 upper panel and TM@bi-NiI_2 lower panel.

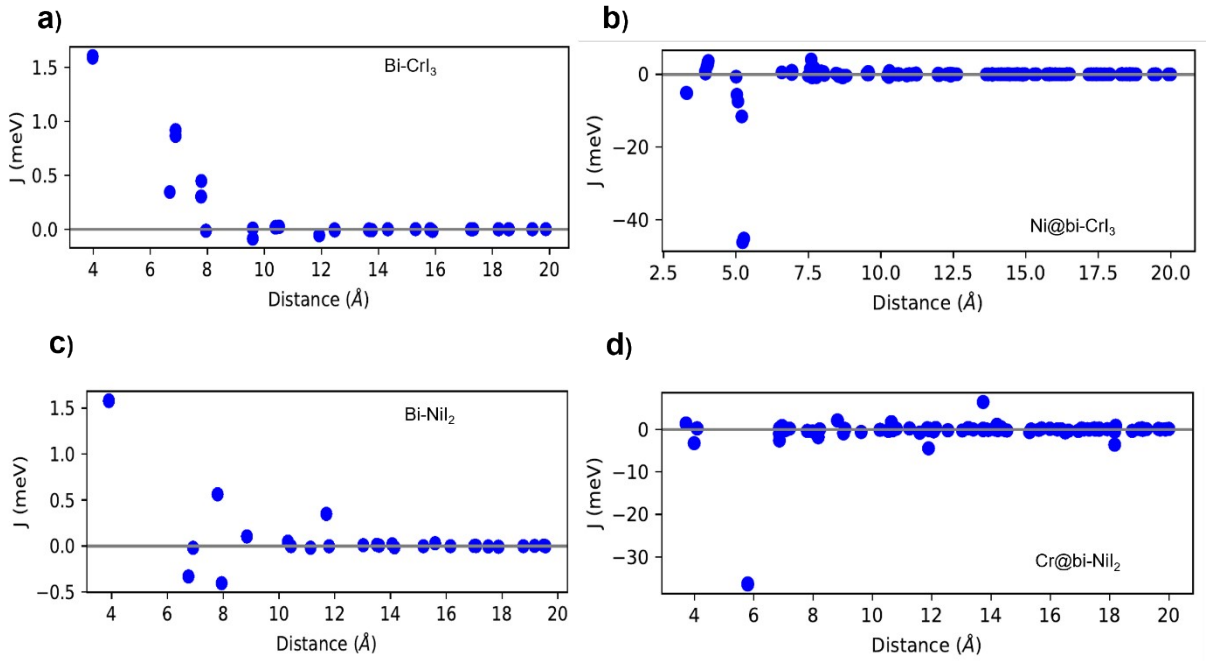

Figure S7. Variation of exchange constant with distance (a) bi-CrI_3 **(b)** Ni@bi-CrI_3 **(c)** bi-NiI_2 **(d)** Cr@bi-NiI_2. Shows that exchange constant is significant till 10 Å. So, we consider 15 Å as a cutoff distance for exchange matrix and T_C calcualtion.

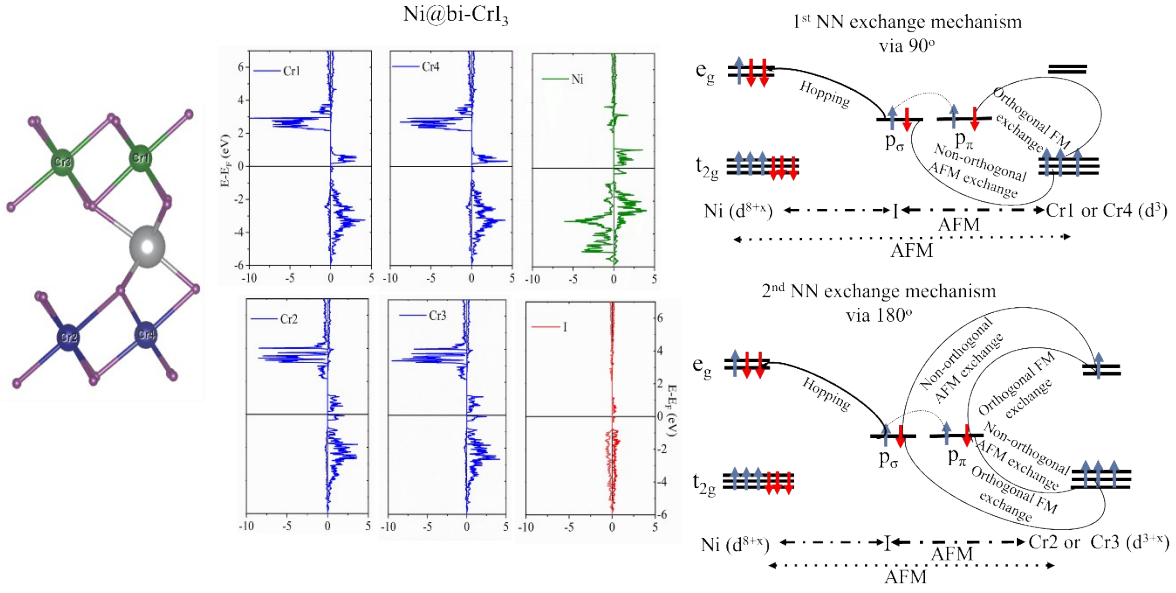

Figure S8. LDOS and exchange mechanism in Ni@bi-CrI_3

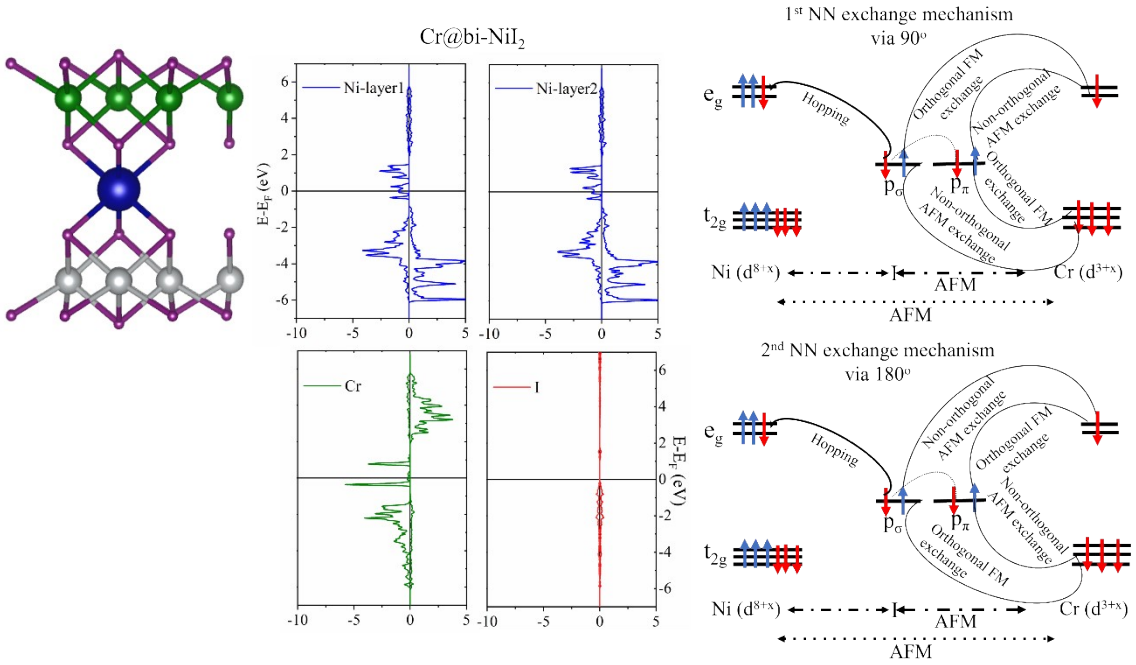

Figure S9. LDOS and exchange mechanism in Cr@bi-NiI_2.

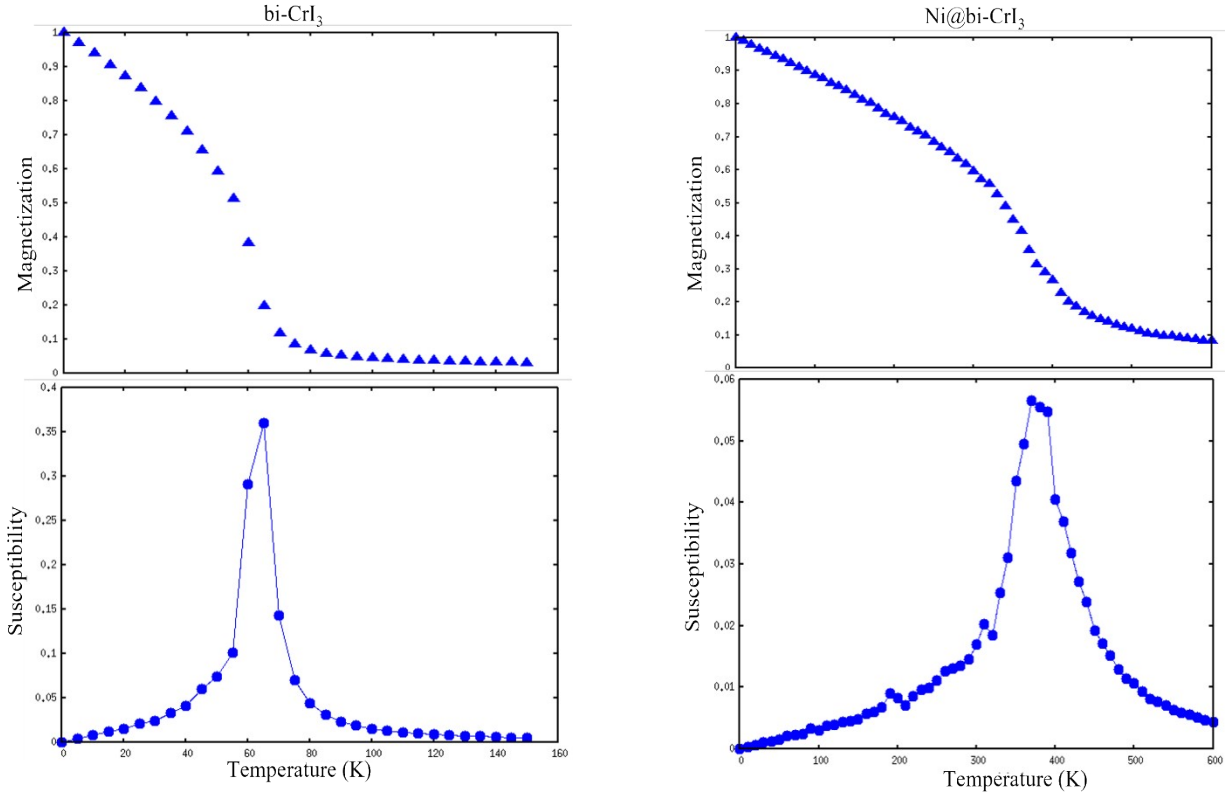

Figure S10. Monte-Carlo (Vampire) simulation of Heisenberg spin hamiltonian for **(left)** bi-CrI_3, **(right)** Ni@bi-CrI_3 using the exchange parameters listed in Tables S3 and S4

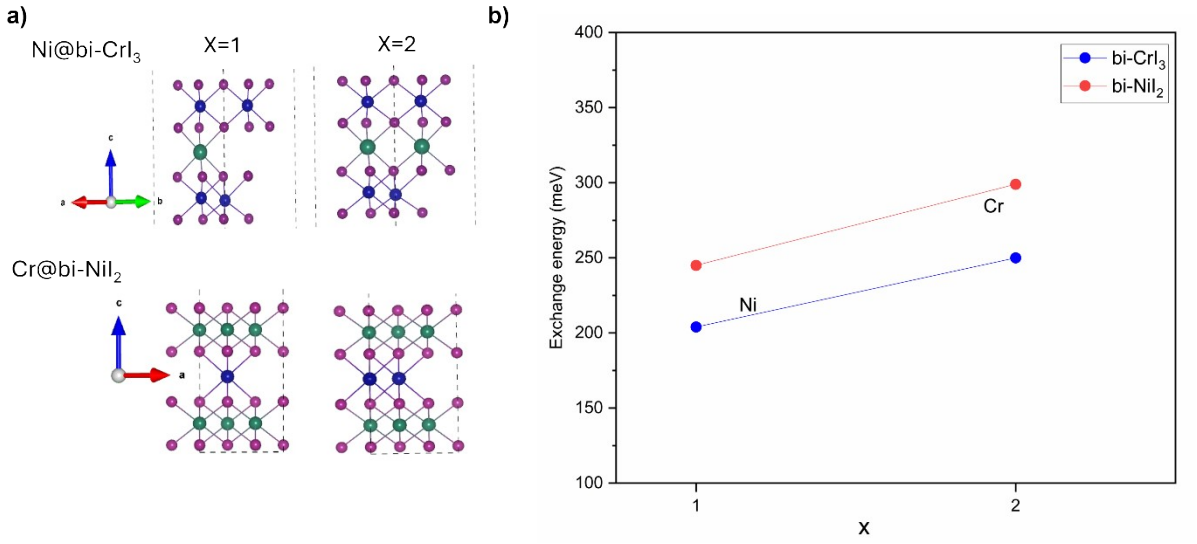

Figure S11. (a) Structures of 1x1 cell and √3×√3 supercell of Ni@bi-CrI_3 and Cr@bi-NiI_2, respectively, with the number of atoms in the supercell increased from one (x=1) to two (x=2), **(b)** Interlayer exchange energies calculated for two densities (x=1,2) of intercalated atoms.

Table S1. Optimized structural properties of bi-CrI_3 and bi-NiI_2

	Calculated	Ref. [1,2]
bi-CrI_3 lattice constant (Å)	6.88	6.89 (1)
Cr-I bond length in bi-CrI_3 (Å)	2.72	2.73 (1)
Interlayer distance in bi-CrI_3 (Å)	3.55	3.55 (1)
Interlayer exchange energy	10.9 meV/u.c.	11 (1)
bi-NiI_2 lattice constant (Å)	3.90	3.93 (2)
Ni-I bond length (Å)	2.71	
Interlayer distance (Å) in bi-NiI_2	3.53	3.51 (2)
Interlayer exchange energy	-9.78 meV/u.c.	11(2)

Table S2. Optimized structural properties of Ni@bi-CrI_3 and Cr@bi-NiI_2

Ni@bi-CrI_3 lattice constant (Å)	a=6.92, b=6.93
Cr-I bond length in Ni@bi-CrI_3 (Å)	2.72
Interlayer distance in Ni@bi-CrI_3 (Å)	3.27
Interlayer exchange energy in Ni@bi-CrI_3	135 meV/u.c.
Cr@bi-NiI_2 lattice constant (Å)	a=b=6.90
Ni-I bond length (Å) in Cr@bi-NiI_2	2.80
Interlayer distance (Å) in Cr@bi-NiI_2	3.69
Interlayer exchange couplingCr@bi-NiI_2	231 meV/u.c.

Table S3. J matrix for different pairs of pristine bi-CrI_3 in meV

	Cr1	Cr2	Cr3	Cr4
Cr1	5.5104	0.9097	4.7574	0.1036
Cr2	0.9097	5.1888	1.3412	4.7576
Cr3	4.7574	1.3412	5.1888	0.9096
Cr4	0.1036	4.7576	0.9096	5.5102

Table S4. J matrix for different pairs of Ni@bi-CrI_3 in meV

	Ni1	Cr1	Cr2	Cr3	Cr4
Ni1	0.000	-6.5285	-59.6473	-59.0012	-6.7458
Cr1	-6.5285	2.9732	1.6059	7.3303	1.9550
Cr2	-59.6473	1.6059	4.3320	6.0943	7.9491
Cr3	-59.0012	7.3303	6.0943	3.5456	2.2412
Cr4	-6.7458	1.9550	7.9491	2.2412	3.0380

Table S5. J matrix for different pairs of bi-NiI_2 in meV

	Ni1	Ni2	Ni3	Ni4	Ni5	Ni6
Ni1	0.0754	6.9058	6.9044	-0.2961	-0.2947	-0.294
Ni2	6.9058	0.0752	6.9058	-0.2945	-0.296	-0.2947
Ni3	6.9044	6.9058	0.0754	-0.294	-0.2947	-0.2962
Ni4	-0.2961	-0.2945	-0.294	0.0756	6.9055	6.9051
Ni5	-0.2947	-0.296	-0.2947	6.9055	0.0756	6.9056
Ni6	-0.294	-0.2947	-0.2962	6.9051	6.9056	0.0756

Table S6. J matrix for different pairs of Cr@bi-NiI_2 in meV

	Cr1	Ni1	Ni2	Ni3	Ni4	Ni5	Ni6
Cr1	0.00	-29.4766	-28.9162	-29.2796	-29.2002	-28.9697	-29.4589
Ni1	-29.4766	-4.0548	-2.7753	-2.7825	0.8284	0.8191	-1.586
Ni2	-28.9162	-2.7753	-3.9142	-2.8798	0.7721	-1.4471	0.8517
Ni3	-29.2796	-2.7825	-2.8798	-3.9098	-1.4227	0.7395	0.8092
Ni4	-29.2002	0.8284	0.7721	-1.4227	-3.9794	-2.8698	-2.6968
Ni5	-28.9697	0.8191	-1.4471	0.7395	-2.8698	-3.847	-2.7928
Ni6	-29.4589	-1.586	0.8517	0.8092	-2.6968	-2.7928	-4.0646

Table S7. U_{eff} values for 3d TM

3d	Sc	Ti	V	Cr	Mn	Fe	Co	Ni	Cu	Zn
U_{eff} (eV)	2.11	2.58	2.72	2.79	3.06	3.29	3.42	3.4	3.87	4.12

References

1. Sivadas, N., Okamoto, S., Xu, X., Fennie, Craig. J., & Xiao, D. Stacking-Dependent Magnetism in Bilayer CrI3. *Nano Lett.* **18**, 7658–7664 (2018).
2. Liu, M. et al. Density Functional Theory Studies on Magnetic Manipulation in NiI2 Layers. *ACS Applied Electronic Materials*, **5**(2), 920–927 (2023).
3. Roome, N. J. & Carey, J. D. Beyond Graphene: stable elemental monolayers of silicene and germanene. *ACS Appl. Mater. Interfaces* **6**(10), 7743–7750 (2014).
4. Skelton, J. M. et al. Influence of exchange-correlation functional on the quasi-harmonic lattice dynamics of II-VI semiconductors. *J. Chem. Phys.* **143**, 064710 (2015).